BRAIN
A JOURNAL OF NEUROLOGY

CSF tau microtubule binding region identifies tau tangle and clinical stages of Alzheimer's disease

Kanta Horie,[1] Nicolas R. Barthélemy,[1] Chihiro Sato[1] and Randall J. Bateman[1,2,3]

Tau is a microtubule associated protein in the brain that aggregates in Alzheimer's disease to form pathological tangles and neurites. Insoluble tau aggregates composed of the microtubule binding region (MTBR) of tau are highly associated with the cognitive and clinical symptoms of Alzheimer's disease. In contrast, levels of soluble forms of tau, such as CSF total tau and phosphorylated tau-181 and tau-217, increase prior to tau aggregation in Alzheimer's disease, but these biomarkers do not measure the MTBR of tau. Thus, how CSF MTBR-tau is altered in Alzheimer's disease remains unclear. In this study, we used sequential immunoprecipitation and chemical extraction methods followed by mass spectrometry to analyse MTBR-tau species in Alzheimer's disease and control CSF. We quantified MTBR-tau-specific regions in the CSF and identified that species containing the region beginning at residue 243 were the most highly correlated with tau PET and cognitive measures. This finding suggests that CSF level of tau species containing the upstream region of MTBR may reflect changes in tau pathology that occur in Alzheimer's disease and could serve as biomarkers to stage Alzheimer's disease and track the development of tau-directed therapeutics.

1 Department of Neurology, Washington University School of Medicine, St. Louis, MO, USA
2 Hope Center for Neurological Disorders, Washington University School of Medicine, St. Louis, MO, USA
3 Charles F. and Joanne Knight Alzheimer's Disease Research Center, Washington University School of Medicine, St. Louis, MO, USA

Correspondence to Randall J. Bateman
Department of Neurology, Washington University School of Medicine
BJC Institute for Health 9603, 425 South Euclid Avenue, St. Louis, MO 63110
E-mail: batemanr@wustl.edu

Introduction

Accumulation of tau protein aggregates in the brain is one of the hallmarks of Alzheimer's disease and other neurodegenerative diseases called tauopathies. Tau pathology appears to propagate across brain regions and spread by the transmission of specific pathological tau species from cell to cell in a prion-like manner although the nature of these species (i.e. monomeric, oligomeric, and fibril species) and the spreading process are uncertain (Frost *et al.*, 2009; Goedert *et al.*, 2010, 2017; Lasagna-Reeves *et al.*, 2012; Sanders *et al.*, 2014; Wu *et al.*, 2016; Mirbaha *et al.*, 2018). In addition, tau has more than 100 potential post-translational modification

sites, including phosphorylation, in addition to multiple truncation sites (Meredith *et al.*, 2013; Sato *et al.*, 2018; Barthélemy *et al.*, 2019; Cicognola *et al.*, 2019; Blennow *et al.*, 2020). Thus, identifying specific pathological tau species involved in tau spread is challenging. Several mass spectrometry (MS) studies suggest that the micro-tubule-binding region (MTBR) of tau is enriched in aggregates in Alzheimer's disease brain (Taniguchi-Watanabe *et al.*, 2016; Roberts *et al.*, 2020). Moreover, a series of cryogenic electron microscopy (cryo-EM) studies demonstrate that the core structure of tau aggregates consists of a subsegment of the MTBR domain and the particular conformation depends on the tauopathy (Fitzpatrick *et al.*, 2017; Falcon *et al.*, 2018, 2019; Zhang *et al.*, 2020). These findings strongly suggest that MTBR-tau is critical for tau aggregation. However, these studies used post-mortem brain tissue. Little is known about the pathophysiology of corresponding extracellular MTBR-containing tau species in CSF, which may serve as a surrogate biomarker of brain tau aggregates in living humans.

CSF is routinely obtained from study participants via lumbar puncture during clinical visits and is widely used to monitor brain changes over the course of neurodegenerative disease. Previous CSF tau biomarker studies suggested that MTBR-tau was missing in CSF and focused on N-terminal and mid-domain regions (Meredith *et al.*, 2013; Sato *et al.*, 2018). The species composed of the N-terminus to mid-domain appear to be actively secreted from neurons into the extracellular space after truncation between the mid- and the MTBR-domain (Sato *et al.*, 2018). Detection of MTBR-tau species were reported (Barthélemy *et al.*, 2016*a*, *b*) but have not been characterized in relationship to disease. Recently, a tau species containing a cleavage at residue 368 (tau368) within the repeat region 4 (R4) was identified in CSF (Blennow *et al.*, 2020), which suggests that it might remain intracellular, enabling aggregation. This species may be a potential biomarker surrogate of tau PET pathology, supporting the hypothesis that tau species containing MTBR in CSF should reflect the underlying tau pathology. However, it is unclear whether tau368 reflects the overall pool of MTBR-tau species given the variations in regions, truncations and conformational structures not captured by antibodies.

In this study, we highlight the presence and potential utility of MTBR-tau species as Alzheimer's disease biomarkers using immunoprecipitation and antibody-independent strategies to analyse CSF tau species. Our results show that a significant amount of MTBR-tau exists in CSF with a C-terminal stub. Moreover, different regions of CSF MTBR-tau stage disease progression and correlate with tau aggregation within the Alzheimer's disease brain. These findings provide new insights into the relationship between MTBR-tau in the brain and CSF and support the use of CSF tau as a fluid biomarker for Alzheimer's disease.

Material and methods

Human brain samples

Discovery cohort

Post-mortem frozen brain tissue samples from two participants with Alzheimer's disease pathology and two control participants without pathology were provided by the Knight ADRC Pathology Core at Washington University School of Medicine. Each sample was classified according to the National Institute on Aging and Alzheimer's Association amyloid stage A3 (Thal phase) for amyloid deposition and Tau Braak stage VI, B3 for tau aggregation. Samples from each participant were collected from 6 to 10 brain regions including the cerebellum, superior frontal gyrus, frontal pole, temporal, occipital, thalamus, amygdala, pons, parietal and striatum.

Validation cohort

Additional post-mortem frozen brain tissue samples from the parietal lobe were analysed from 20 participants (eight amyloid-negative and 12 amyloid-positive by CSF amyloid-β 42/40 ratios) as a validation cohort. The 12 amyloid-positive samples were further divided into clinical groups according to their Clinical Dementia Rating (CDR) scores, and classified as very mild to moderate Alzheimer's disease (amyloid-positive, CDR = 0.5–2, $n = 5$) or severe Alzheimer's disease (amyloid-positive, CDR = 3, $n = 7$). These human studies were approved by the Washington University Institutional Review Board.

Human CSF samples

Cross-sectional cohort

CSF samples from 100 participants were collected from the amyloid-β stable isotope labelling kinetics (SILK) study (Patterson *et al.*, 2015) for analysis as a cross-sectional cohort. CSF collection was performed as previously described (Patterson *et al.*, 2015). Briefly, CSF was collected at baseline. Next, participants received a leucine bolus infusion over 10 min. Six millilitres of CSF was obtained hourly for 36 h. CSF aliquots collected at Hour 30 were used for MS measurement of tau species in this study. Amyloid status was defined using CSF amyloid-β 42/40 ratio as previously reported (Patterson *et al.*, 2015). The corresponding cut-off ratio (0.1389) maximized the accuracy in predicting amyloid-positivity as determined by Pittsburgh compound B (PiB) PET. Amyloid groups were further divided into clinical groups according to their CDR scores as shown in Table 1.

Longitudinal cohort

From the cross-sectional cohort, 28 participants (14 amyloid-positive and 14 amyloid-negative) were followed for 2 to 9 years to assess the longitudinal trajectory of tau species in CSF. CSF samples were collected and analysed in the same manner as the cross-sectional cohort.

Table 1 Demographics and biomarkers values of CSF study participants

Variable	Cross-sectional cohort (n = 100)					Longitudinal cohort (n = 28)		Tau PET cohort (n = 35)	
	Control	Preclinical AD	Very mild AD	Mild-moderate AD	Non-AD CI	Control	AD	Control	AD
n	30	18	28	12	12	14	14	15	20
Age	71 (5)	73 (7)	75 (7)	72 (8)	75 (8)	74 (5)	77 (6)	75 (6)	75 (6)
Gender, female/male	18/12	11/7	11/17	2/10	2/10	5/9	7/7	12/3	11/9
CDR	0	0	0.5	1–2 ($\geqslant$1)	0.5–1 ($\geqslant$0.5)	0–0.5	0–2	0–0.5	0–2
CSF amyloid-β 42/40	0.18 (0.02)	0.10 (0.02)	0.09 (0.02)	0.10 (0.02)	0.17 (0.02)	NA	NA	NA	NA
PiB SUVR[a]	1.04 (0.11) [27]	1.99 (0.87) [16]	3.14 (0.92) [13]	2.73 (2.10) [2]	0.98 (0.05) [5]	1.11 (0.18) [13]	2.47 (0.59) [11]	1.10 (0.13) [10]	2.37 (0.34) [14]
AV45 SUVR[a]	1.12 (0.42) [16]	1.85 (0.52) [8]	2.18 (0.53) [6]	2.41 (na) [1]	0.96 (0.15) [2]	0.98 (0.19) [9]	2.10 (0.46) [12]	0.98 (0.26) [13]	2.09 (0.49) [18]
Amyloid status	Negative	Positive	Positive	Positive	Negative	Negative	Positive	Negative	Positive
AV-1451 SUVR	NA	NA	NA	NA	NA	NA	NA	1.23 (0.14)	1.75 (0.69)
CSF tau level, ng/ml									
MTBR-tau-243	2.44 (0.63)	4.47 (3.51)	6.18 (2.71)	9.17 (5.32)	2.75 (0.89)	2.94 (0.87)	7.09 (4.76)	2.70 (0.67)	6.82 (4.26)
MTBR-tau-299	0.39 (0.13)	0.80 (0.45)	1.14 (0.42)	1.00 (0.49)	0.45 (0.17)	0.44 (0.23)	1.18 (0.47)	0.40 (0.21)	1.07 (0.31)
MTBR-tau-354	2.20 (0.41)	2.73 (0.79)	3.21 (0.77)	2.73 (0.80)	2.31 (0.49)	2.24 (0.48)	3.61 (0.89)	2.33 (0.64)	3.43 (0.72)

Data are presented as mean (SD). Amyloid statuses in longitudinal and tau PET cohorts were determined historically from the results of the cross-sectional cohort and amyloid PET, respectively. The concentration of each MTBR-tau isoform (MTBR-tau-243, MTBR-tau-299, and MTBR-tau-354) was determined by mass spectrometry following to chemical extraction method in post-immunoprecipitated CSF samples. AD = Alzheimer's disease; AV-1451 = flortaucipir; AV-45 = florbetapir; CI = cognitive impairment; NA = not available; PiB = Pittsburgh compound B.

[a]Values in square brackets indicate the number of available measures within the group.

Tau PET cohort

Thirty-five participants (20 amyloid-positive and 15 amyloid-negative, including 16 participants from longitudinal cohort) had tau PET AV-1451 standardized uptake value ratio (SUVR) measures within 3 years from the time of CSF collection. PET scans were performed as previously described (Sato *et al.*, 2018) and the partial-volume correction was performed for SUVR using a regional spread function technique (Su *et al.*, 2015). CSF samples were collected and analysed in the same manner as the other cohorts.

Mass spectrometry

Brain tau analysis

Frozen brain tissue samples were sliced using a cryostat at –20°C and collected in tubes. The tissue (300–400 mg) was sonicated in ice-cold buffer containing 25 mM Tris-hydrochloride (pH 7.4), 150 mM sodium chloride, 10 mM EDTA, 10 mM EGTA, phosphatase inhibitor cocktail, and protease inhibitor cocktail at a concentration of 0.3 mg/μl of brain tissue. The homogenate was clarified by centrifugation for 20 min at 11 000*g* at 4°C. The supernatant (whole brain extract) was aliquoted into new tubes and kept at –80°C until use. The whole brain extract was incubated with 1% sarkosyl for 60 min on ice, followed by ultra-centrifugation at 100 000*g* at 4°C for 60 min to obtain an insoluble pellet. The insoluble pellet was resuspended with 200 μl of PBS followed by sonication and the insoluble suspension was kept at –80°C until use.

For whole brain tau analysis, tau species in whole brain extract were immunoprecipitated with Tau1 and HJ8.5 antibodies. The immunoprecipitated tau species were processed and digested as described previously (Sato *et al.*, 2018).

For insoluble tau analysis, insoluble suspension (10–20 μl containing 2.5 μg of total protein) was mixed with 200 μl of lysis buffer {7 M urea, 2 M thio-urea, 3% 3-[(3-cholamidopropyl)dimethylammonio]-1-propanesulfonate, 1.5% *n*-octyl glucoside, 100 mM triethyl ammonium bicarbonate (TEABC)} followed by spiking with 5 μl of solution containing [15]N Tau-441(2N4R) Uniformly Labeled (2 ng/μl, gift from Dr Guy Lippens, Lille University, France) as an internal standard. Five microlitres of 500 mM dithiothreitol was added to the suspension, followed by sonication. The resulting solution was mixed with 15 μl of 500 mM iodoacetamide and incubated for 30 min at room temperature in the dark. Protein digestion was conducted using the filter-aided sample preparation method as previously reported (Roberts *et al.*, 2020). Briefly, each prepared solution was loaded on a Nanosep 10K filter unit (PALL) and centrifuged. After washing the sample on the filter unit with 8 M urea in 100 mM TEABC solution, immobilized proteins were digested on the filter using 0.25 μg of endoproteinase Lys-C at 37°C for 60 min. Then, the samples were further digested using 0.4 μg trypsin at 37°C overnight.

The digested samples (whole brain tau and insoluble tau species) were collected by centrifugation, then desalted by C18 TopTip (Glygen). In this purification process, 50 fmol each of AQUA internal-standard peptide for residues 354-369 (MTBR-tau-354) and 354-368 (tau368) was spiked for the differential quantification. Before eluting samples, 3% hydrogen peroxide and 3% formic acid (FA) in water were added onto the beads, followed by overnight incubation at 4°C to oxidize the peptides containing methionine. The eluent was lyophilized and resuspended in 27.5 μl of 2% acetonitrile and 0.1% FA in water prior to MS analysis on nanoAcquity UPLC system (Waters) coupled to Orbitrap Fusion™ Tribrid™ or Orbitrap Tribrid™ Eclipse™ (Thermo Scientific) operating in parallel reaction monitoring (PRM) mode.

Sixteen brain tau peptides from both whole brain tau and insoluble tau species were quantified by comparison with corresponding isotopomer signals from the ^{15}N or AQUA internal standard (Supplementary Table 1). Peptide-profile comparisons across brain samples were performed by normalizing each peptide amount by a mid-domain tau peptide (residue 181-190).

CSF tau analysis

CSF (455 μl) was mixed with 10 μl of solution containing [15]N Tau-441(2N4R) Uniformly Labeled (100 pg/μl) as an internal standard. The tau species consisting primarily of N-terminal to mid-domain regions were immunoprecipitated with Tau1 and HJ8.5 antibodies. Immunoprecipitated tau species were processed and digested as described previously (Sato *et al.*, 2018). Subsequently, 20 μl of ^{15}N-tau internal standard (100 pg/μl) was spiked into the post-immunoprecipitated CSF. Then, tau was chemically extracted as previously reported (Barthélemy *et al.*, 2016b) with some modifications. Highly abundant CSF proteins were precipitated using 25 μl of perchloric acid. After mixing and incubation on ice for 15 min, the mixture was centrifuged at 20 000*g* for 15 min at 4°C, and the supernatant was further purified using the Oasis HLB 96-well μElution Plate (Waters) according to the following steps. The plate was washed once with 300 μl of methanol and equilibrated once with 500 μl of 0.1% FA in water. The supernatant was added to the Oasis HLB 96-well μElution Plate and adsorbed to the solid phase. Then, the solid phase was washed once with 500 μl of 0.1% FA in water. Elution buffer (100 μl; 35% acetonitrile and 0.1% FA in water) was added, and the eluent was dried by SpeedVac. Dried sample was dissolved by 50 μl of trypsin solution (10 ng/μl) in 50 mM TEABC and incubated at 37°C for 20 h.

After incubation for both immunoprecipitated and chemically extracted samples, each tryptic digest was purified by solid phase extraction on C18 TopTip. In this purification process, 5 fmol each of AQUA internal-standard peptide for residues 354-369 (MTBR-tau-354) and 354-368 (tau368) was spiked for the differential quantification. Before eluting samples, 3% hydrogen peroxide and 3% FA in water were added to the beads, followed by overnight incubation at 4°C to oxidize the peptides containing methionine. The eluent was lyophilized and resuspended in 27.5 μl of 2% acetonitrile and 0.1% FA in water prior to MS analysis on a

nanoAcquity UPLC system coupled to Orbitrap Fusion[TM] Lumos[TM] Tribrid[TM] or Orbitrap Tribrid[TM] Eclipse[TM] mass spectrometer (Thermo Scientific) operating in PRM mode. Nineteen CSF tau peptides were quantified (Supplementary Table 1). The schematic procedure of CSF tau analysis is described in Supplementary Fig. 1.

Statistical analysis

Differences in biomarker values were assessed with one-way ANOVAs, unless otherwise specified. A two-sided $P < 0.05$ was considered statistically significant and corrected for multiple comparisons using Benjamini-Hochberg false discovery rate (FDR) method with FDR set at 5% (Benjamini and Hochberg, 1995). Spearman correlations were used to assess associations between tau biomarkers and cognitive testing measures and tau PET SUVR.

Data availability

The authors confirm that the data supporting the findings of this study are available within the article and its Supplementary material.

Results

Enrichment profiling of tau species in Alzheimer's disease brain

We hypothesized that tau aggregation in Alzheimer's disease brain would be reflected in tau profiles in CSF. Therefore, we first analysed tau profiles in insoluble extracts from Alzheimer's disease and control brains (Fig. 1B, discovery cohort) to later compare with CSF tau profiles. We identified that the species containing residues 299-317 (MTBR-tau-299) and 354-369 (MTBR-tau-354), located between R2 and R3 domains and within the R4 domain, respectively, were more enriched in the insoluble extract from Alzheimer's disease brain than control by 3–4-fold. The upstream region of MTBR residue 243-254 (MTBR-tau-243) was also about three times greater in Alzheimer's disease brain as compared to the control, while species containing residues 260-267 and 275-280 located within R1 and R2 domains, respectively, did not differ between Alzheimer's disease and control tissues. No other regions of tau were enriched in Alzheimer's disease brain compared to controls. Of note, no change was observed for the identified MTBR-tau species in whole brain tau (whole brain extract) between control and Alzheimer's disease (Supplementary Fig. 2A).

These results were reproduced in brain samples from control (amyloid-negative, $n = 8$), very mild to moderate Alzheimer's disease (amyloid-positive, CDR = 0.5–2, $n = 5$) and severe Alzheimer's disease (amyloid-positive, CDR = 3, $n = 7$) participants (Fig. 1C and Supplementary Fig. 2B, validation cohort), which suggested MTBR-tau-243, 299, and 354 species were specifically enriched in insoluble tau

aggregates over the stages of disease progression. In the validation cohort, other species including residues 6-23 (N-terminal domain), 151-155 (mid-domain), and 275-280 (R2 domain) in insoluble tau aggregates also showed significant enrichment in severe Alzheimer's disease brain, but the increments were moderate (<2-fold). Notably, the species containing residues 195-209 and 226-230 within the mid-domain were significantly lower in Alzheimer's disease brain compared to the control, likely the result of extensive hyper-phosphorylation occurring on residues 199, 202, 205, 208, and 231 in insoluble tau aggregates (Malia et al., 2016; Neddens et al., 2018).

Next, we examined the recently reported truncated tau368 (residue 354-368) species generated by asparagine endopeptidase (Zhang et al., 2014; Blennow et al., 2020) against its paired non-truncated species, MTBR-tau-354, and quantified both species in brain insoluble extracts (Supplementary Fig. 3). We found a high correlation between tau368 and MTBR-tau-354 ($r = 0.9783$), suggesting that truncation at residue 368 occurs at the same rate in different stages of brain pathology.

Quantification of MTBR-tau in CSF

To determine whether the enrichment of MTBR-tau in Alzheimer's disease brain aggregates are related to levels of soluble tau species in the CSF, we developed a method to analyse MTBR-tau in CSF. The method utilizes tau chemical extraction in post-immunoprecipitated (Tau1/HJ8.5) CSF followed by MS analysis (Supplementary Fig. 1), which provided sufficient recovery for quantifying MTBR peptides (Supplementary Fig. 4). Tau peptide abundance recovered by Tau1/HJ8.5 immunoprecipitation method before chemical extraction was dramatically decreased after residue 222; therefore, peptides from the N-terminal to mid-domain tau (residues 6-23 to 243-254) were recovered by the immuno-precipitation method (Sato et al., 2018). In contrast, the concentrations of MTBR-tau species quantified by the chemical extraction method were relatively low compared to the N-terminus to mid domain regions but still comparable to the other regions of tau by immunoprecipitation (Fig. 2). CSF concentrations from normal control participants (calculated as total values from immunoprecipitation and chemical extraction methods) ranged from 8.2 to 32.0 ng/ml for mid-domain species (residues 151-155, 181-190, 195-209, and 212-221), 0.4 to 3.7 ng/ml for MTBR-tau species (residues 243-254, 260-267, 275-280, 282-290, 299-317, and 354-369), and 6.5 and 5.1 ng/ml for non-MTBR C-terminal tau species (residues 386-395 and 396-406). The CSF concentrations of C-terminal-containing truncated tau species were in a similar range as those containing the mid-domain (residues 195-209 and 212-221), suggesting the C-terminal side of tau is also truncated in neuronal cells and secreted extracellularly in the same manner as N-terminus to mid-domain tau (Sato et al., 2018).
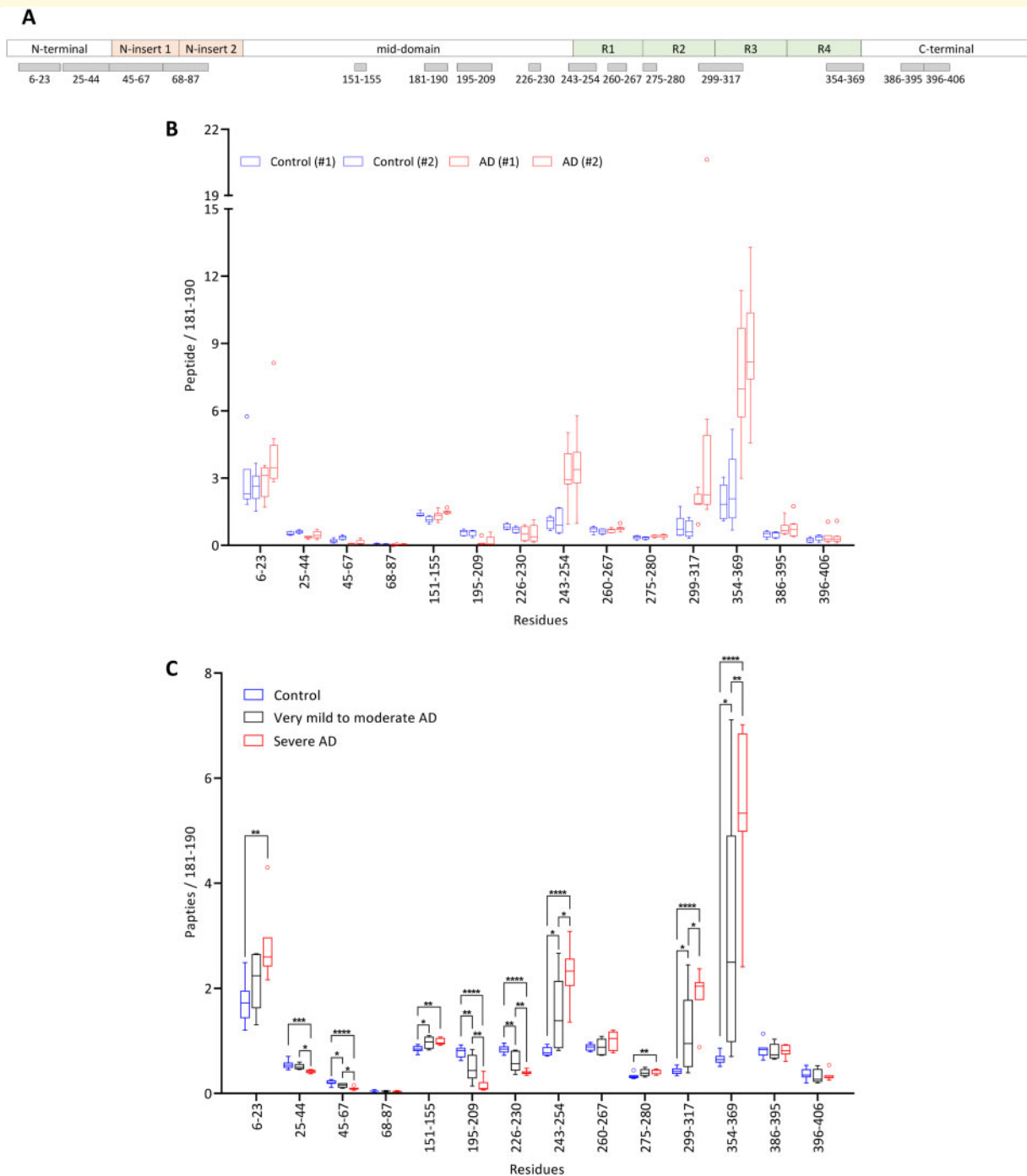
Figure 1 Brain MTBR-tau-243, 299 and 354 species are enriched in aggregated Alzheimer's disease brain insoluble extracts compared to control brain extracts, confirming that MTBR-tau is specifically deposited in Alzheimer's disease brain.
(**A**) Schematic of the quantified peptides from tau (grey bars), (**B**) the enrichment profile of tau peptides from control and Alzheimer's disease brains ($n = 2$ with six to eight brain regions samples/group in discovery cohort) and (**C**) the enrichment profile of tau peptides from control (amyloid-negative, $n = 8$), very mild to moderate Alzheimer's disease (AD) (amyloid-positive, CDR = 0.5–2, $n = 5$), and severe Alzheimer's disease brains (amyloid-positive, CDR = 3, $n = 7$) (total $n = 20$ in validation cohort). The relative abundance of tau peptides was quantified relative to the mid-domain (residue 181-190) peptide for internal normalization. The species containing the upstream region of the MTBR domain (residue 243-254, MTBR-tau-243) and repeat region 2 (R2) to R3 and R4 (residues 299-317, MTBR-tau-299 and 354-369, MTBR-tau-354, respectively) were highly enriched in the insoluble fraction from Alzheimer's disease brains compared to controls and were specifically enriched by clinical stage of disease progression as measured by the CDR. MTBR-tau-299 and MTBR-tau-354 are located inside the filament core, whereas MTBR-tau-243 is located outside the core of Alzheimer's disease aggregates (Fitzpatrick et al., 2017). Of note, residue 195-209 was decreased in Alzheimer's disease brains, potentially due a high degree of phosphorylation. Data are represented as box-and-whisker plots with Tukey method describing median, interquartile interval, minimum, maximum, and individual points for outliers. Significance in statistical test: ****$P < 0.001$, ***$P < 0.001$, **$P < 0.01$, *$P < 0.05$.
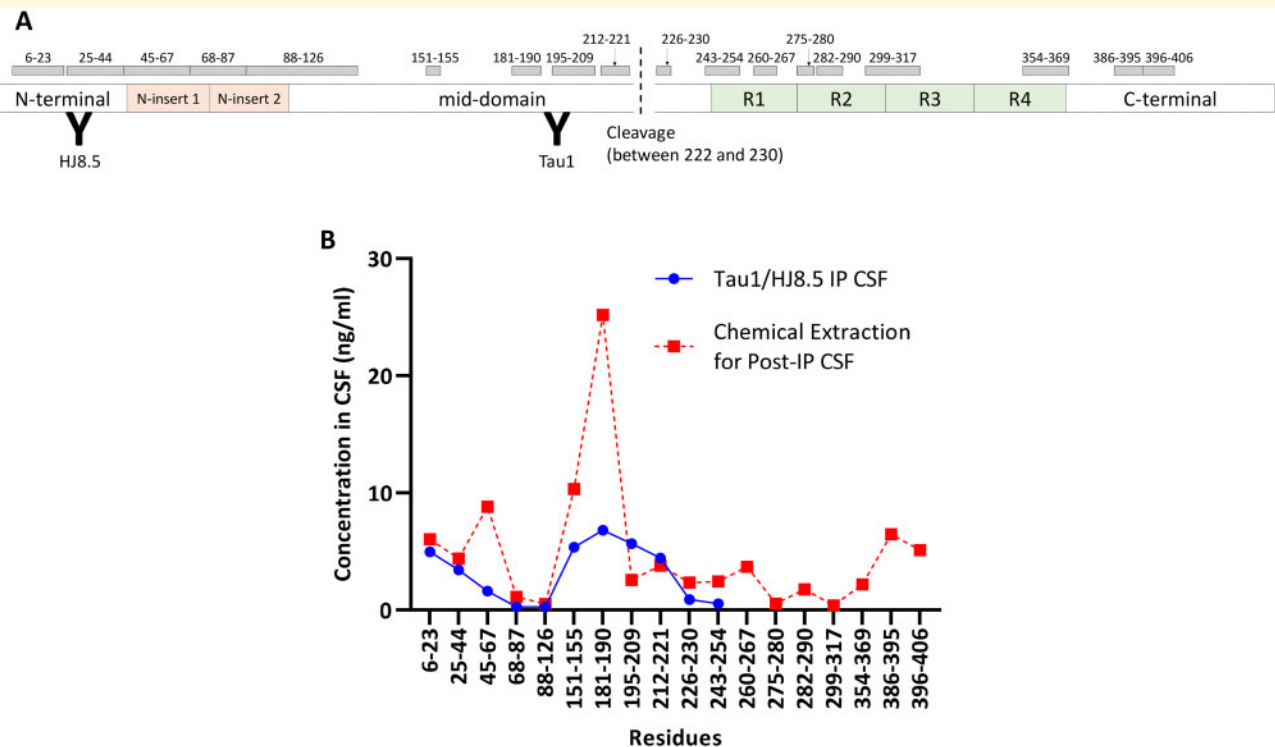
Figure 2 Chemical extraction after immunoprecipitation by Tau1/HJ8.5 reveals whole tau profiles in CSF. (**A**) Schematic of quantified tau peptides and sample preparation procedure and (**B**) the tau profile in control human CSF. Tau peptides in control human CSF from a cross-sectional cohort of amyloid-negative and CDR = 0 patients ($n = 30$) were quantified by Tau1/HJ8.5 immunoprecipitation focusing on N-terminal to mid-domain tau. To quantify the species containing the MTBR and C-terminal region, post-immunoprecipitated (Post-IP) CSF samples were chemically extracted and analysed sequentially. Using the Tau1/HJ8.5 immunoprecipitation method (blue circle), peptide recovery dramatically decreased after residue 222; therefore, only N-terminal to mid-domain tau (residues 6-23 to 243-254) peptides were quantified by this method (Sato *et al.*, 2018). In contrast, the chemical extraction method of post-immunoprecipitated CSF (red square) enabled quantification of whole regions of tau including the MTBR to C-terminal regions at concentrations between 0.4 and 7 ng/ml. Data are represented as means.

CSF MTBR-tau in an Alzheimer's disease cross-sectional cohort

To determine whether MTBR-containing species present in the extracellular space reflect Alzheimer's disease-related changes, we analysed CSF from a cross-sectional cohort of amyloid-negative and amyloid-positive participants at different clinical stages: amyloid-negative CDR = 0 (control, $n = 30$), amyloid-positive CDR = 0 (preclinical Alzheimer's disease, $n = 18$), amyloid-positive CDR = 0.5 (very mild Alzheimer's disease, $n = 28$), amyloid-positive CDR $\geqslant 1$ (mild-moderate Alzheimer's disease, $n = 12$), and amyloid-negative CDR $\geqslant 0.5$ (non-Alzheimer's disease cognitive impairment, $n = 12$).

First, we investigated CSF levels of three MTBR-tau species specifically enriched in Alzheimer's disease brain (MTBR-tau-243, MTBR-tau-299, and MTBR-tau-354) (Fig. 3). All three species were present in both Alzheimer's disease and control CSF and levels were greater in the amyloid-positive groups even for the asymptomatic stage (CDR = 0) when compared to the control group (MTBR-tau-243 $P = 0.0170$, MTBR-tau-299 $P = 0.0002$, and MTBR-tau-354 $P = 0.0076$). Remarkably, these species had distinct

characteristics in CSF after clinical disease onset. MTBR-tau-299 levels were 204% higher in preclinical Alzheimer's disease compared to controls but saturated between very mild Alzheimer's disease (CDR = 0.5) and mild-moderate Alzheimer's disease (CDR $\geqslant 1$) ($P = 0.2541$), while MTBR-tau-354 levels were significantly lower in samples collected post-symptom onset ($P = 0.0345$). In contrast, MTBR-tau-243 levels were incrementally higher across all disease stages including after symptom onset ($P = 0.0025$). These results suggest that the regional specificity even within the MTBR-tau species can distinguish among different Alzheimer's disease stages and that MTBR-tau-243 is a good Alzheimer's disease stage-specific marker.

Next, we investigated whether CSF MTBR-tau species provide enhanced sensitivity and specificity in staging Alzheimer's disease when compared to tau species containing other regions. We quantified multiple species containing N-terminal, mid-domain, MTBR, and C-terminal domains by region-specific methods (Supplementary Figs 5–7). N-terminal to mid-domain species were quantified by immunoprecipitation as well as chemical extraction for post-immunoprecipitated CSF, while the MTBR to
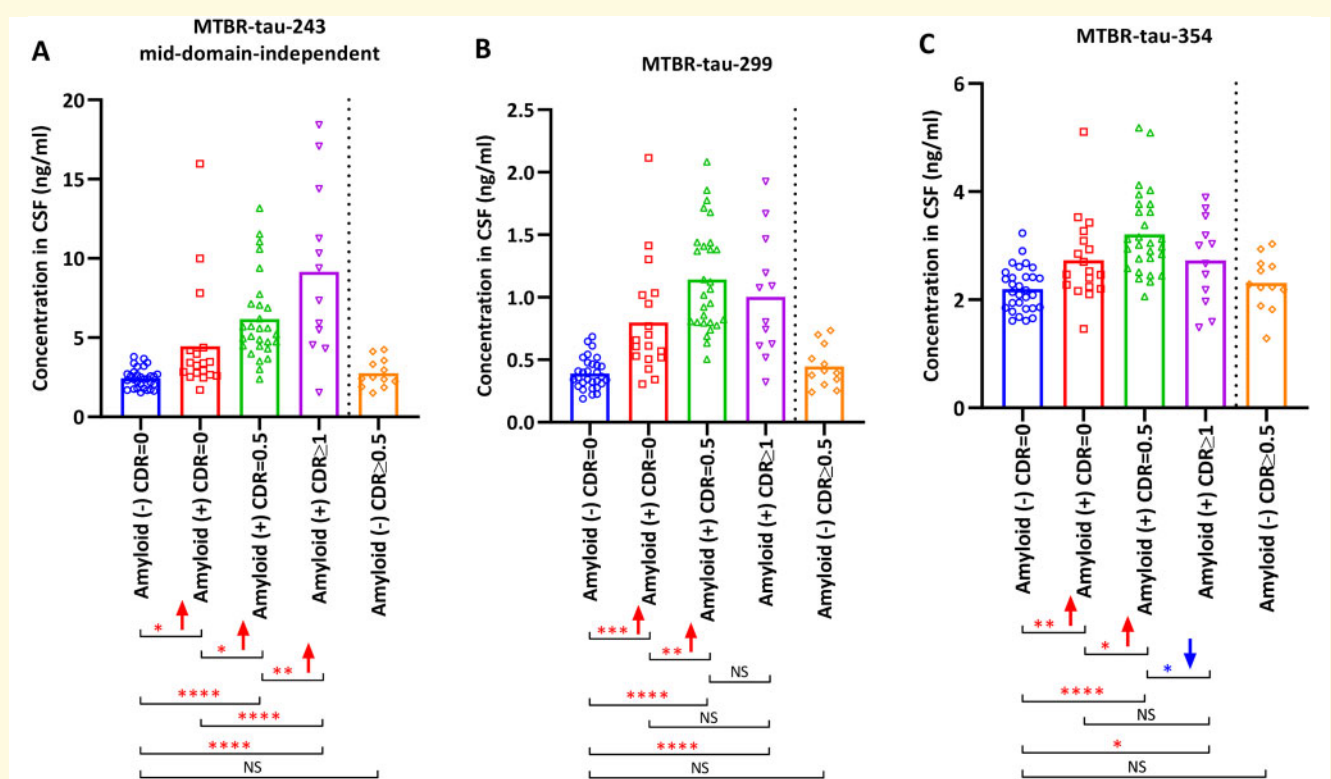
Figure 3 CSF MTBR-tau-243, 299, and 354 species exhibited different profiles to amyloid plaques and clinical dementia stage.
Mid-domain-independent tau peptides (**A**) MTBR-tau-243, (**B**) MTBR-tau-299, and (**C**) MTBR-tau-354 concentrations in post-immunoprecipitated CSF using chemical extraction method from the cross-sectional cohort. Amyloid-negative CDR = 0 (control, n = 30), amyloid-positive CDR = 0 (preclinical Alzheimer's disease, n = 18), amyloid-positive CDR = 0.5 (very mild Alzheimer's disease, n = 28), amyloid-positive CDR $\geqslant$ 1 (mild-moderate Alzheimer's disease, n = 12), and amyloid-negative CDR $\geqslant$ 0.5 (non-Alzheimer's disease cognitive impairment, n = 12). Mid-domain-independent MTBR-tau-243 showed a continuous increase with Alzheimer's disease progression through all clinical stages. MTBR-tau-299 and MTBR-tau-354 concentrations similarly increased until the very mild Alzheimer's disease stage (amyloid-positive and CDR = 0.5), but then either saturated (MTBR-tau-299) or decreased (MTBR-tau-354) at CDR $\geqslant$ 1. The P-values in red or blue fonts indicate a significant increase or decrease, respectively. Data are represented as the individual results (plots) and the mean (bar). Significance in statistical test: ****$P < 0.001$, ***$P < 0.001$, **$P < 0.01$, *$P < 0.05$. NS = not significant.

C-terminal species were quantified only by the chemical extraction method for post-immunoprecipitated CSF because quantifiable signals were not obtained by immuno-precipitation. Levels of species containing N-terminal domains quantified by the immunoprecipitation method were not different between the control and asymptomatic stage (except for residue 6-23, P = 0.0362) or other neighbouring disease stages. The mid-domain species levels by the immunoprecipitation method were significantly greater in the asymptomatic amyloid stage than in controls (except for residue 212-221, P = 0.0762) but the effect size was relatively modest (123%–168% versus control) compared to the MTBR-tau species (e.g. MTBR-tau-299 levels were >200% greater at the pre-clinical Alzheimer's disease stage than control) and did not differ across later disease stages. Regardless of the extraction method (the combination of Tau1/HJ8.5 immunoprecipitation and chemical extraction for post-immunoprecipitated CSF, or chemical extraction alone for post-immunoprecipitated CSF), MTBR-tau-243, 299,

and 354 species showed greater differences between control and disease stages compared to N-terminal to mid-domains species (residues 6-23 to 226-230, Supplementary Figs 7 and 8). Profiles from the other species containing MTBR to C-terminal domains (residues 260-267, 275-280, 282-290, 386-395, and 396-406) were similar to the mid-domain species and were not specific for the stage of Alzheimer's disease clinical dementia.

In summary, the three representative species containing MTBR (MTBR-tau-243, MTBR-tau-299, and MTBR-tau-354) that were enriched in Alzheimer's disease brain (Fig. 1) had particular characteristics in CSF with MTBR-tau-243 exhibiting the greatest specificity to Alzheimer's disease dementia stage. Of note, a high correlation was observed between the tau368 truncated form and MTBR-tau-354 non-truncated form in CSF (r = 0.8382) (Supplementary Fig. 9). The only species that could reliably distinguish the clinical stages of Alzheimer's disease was MTBR-tau-243.

Mid-domain-independent MTBR-tau-243 as a specific biomarker to stage Alzheimer's disease

The incrementally greater levels of the MTBR-tau-243 species across Alzheimer's disease clinical dementia stages suggests it may be a reliable predictor of disease progression. We investigated which MTBR-tau species (MTBR-tau-243, MTBR-tau-299, and MTBR-tau-354) had the highest correlations with results of cognitive tests such as CDR-sum of boxes (CDR-SB) and the Mini-Mental State Examination (MMSE). We found that the mid-domain-independent MTBR-tau-243 species in the amyloid-positive group was highly correlated with both CDR-SB and MMSE ($r = 0.5562$, $P < 0.0001$ and $r = -0.5433$, $P < 0.0001$, respectively) (Supplementary Figs 10 and 11). Other species levels had much lower or no significant correlations with the cognitive testing (Supplementary Table 2), which suggests that CSF MTBR-tau-243 specifically differentiates clinical stage and global disease progression from the asymptomatic stage through advancing clinical stages of Alzheimer's disease.

CSF MTBR-tau in an Alzheimer's disease longitudinal cohort

From the cross-sectional cohort, a subset of participants ($n = 28$) were followed for 2 to 9 years to measure the longitudinal trajectory of MTBR-tau in CSF (Supplementary Table 3). MTBR-tau species enriched in Alzheimer's disease brain (MTBR-tau-243, MTBR-tau-299, and MTBR-tau-354) were significantly increased over time in the amyloid-positive group ($P < 0.01$ by two-tailed paired t-test between first and second visits) but not the amyloid-negative group, except for MTBR-tau-243 (Supplementary Fig. 12). The amyloid-negative group also showed slight longitudinal increases of MTBR-tau-243 but lower than observed for the amyloid-positive group (means of differences = 0.4926 and 2.208 in amyloid-negative and positive groups, respectively).

Figure 4 shows the longitudinal change-rates of the MTBR-tau species concentrations in individual participants. Notably, one participant (Participant A) with the highest CDR after disease onset (CDR change from 1 to 2 in 7 years) showed specific trajectory profiles for each MTBR-tau species. MTBR-tau-243 continuously increased even from mild Alzheimer's disease (CDR = 1) to moderate Alzheimer's disease (CDR = 2), while MTBR-tau-299 and MTBR-tau-354 showed a decrease in this participant's CSF after mild Alzheimer's disease. Other participants in the amyloid-positive group were classified as preclinical Alzheimer's disease or very mild Alzheimer's disease (CDR = 0 or 0.5, respectively) at the first visit, and the increasing trend for each species level was seen for most of the participants, which supports the findings from the cross-sectional cohort.

Correlation with tau PET imaging

Tau pathology as measured by tau PET scans correlates strongly with cognitive decline and clinical stage of Alzheimer's disease (Arriagada et al., 1992; Johnson et al., 2016; Ossenkoppele et al., 2016; Bejanin et al., 2017; Jack et al., 2018; Gordon et al., 2019). Here, we investigated whether MTBR-tau in CSF was correlated with brain tau pathology measured by tau PET (Fig. 5). Mid-domain-independent MTBR-tau-243 significantly correlated with tau PET SUVR ($r = 0.7588$, $P < 0.0001$), while MTBR-tau-299 and MTBR-tau-354 were much less correlated ($r = 0.4584$, $P = 0.0056$ and $r = 0.4375$, $P = 0.0086$, respectively). Tau species containing residue 226-230 also showed high correlation with tau PET SUVR ($r = 0.6248$, $P < 0.0001$; Supplementary Table 4), but lower than observed for MTBR-tau-243. This suggests that CSF MTBR-tau-243 and the surrounding region may be surrogate biomarkers of tau aggregation in the brain. The ability to specifically and quantitatively track tau pathology in the brain is a much-needed biomarker for Alzheimer's disease clinical studies.

Discussion

MTBR regions of tau have been investigated primarily in brain aggregates but not extensively in CSF. In this study, using a sensitive and antibody-independent method to analyse CSF tau, we show the presence and quantification of MTBR regions of tau in CSF samples from human participants. Past studies utilizing antibody-dependent assays (Meredith et al., 2013; Sato et al., 2018) may have failed to detect MTBR-containing tau species in CSF due to assay limitations including antibody specificity or sensitivity, or the ability to recover potential conformations adopted by MTBR species in CSF. Alternatively, MTBR-tau may be truncated by various proteases, generating fragments that are not detected in conventional immunoassays or immunoprecipitation followed by MS assays (Gamblin et al., 2003; Cotman et al., 2005; Zhang et al., 2014; Zhao et al., 2016; Chen et al., 2018; Quinn et al., 2018). In this study, we measured surprisingly robust concentrations of MTBR-tau species, at about 1% to 10% compared to the mid-domain tau species by using a chemical extraction method followed by mass spectrometry (Fig. 2 and Supplementary Fig. 1).

To date, it has been unclear whether MTBR-tau could be involved in extracellular tau propagation because extracellular levels were thought to be too low to seed and spread the pathology. Our new findings of the stoichiometry of MTBR in CSF supports the hypothesis that MTBR-containing species could spread extracellularly as pathological species. These measures also inform potential targets of anti-tau drugs in development for Alzheimer's disease and provide a quantitative measure of the target as shown by the 2–3-fold increase of MTBR-tau species in CSF from patients with Alzheimer's disease. However, a limitation is that the
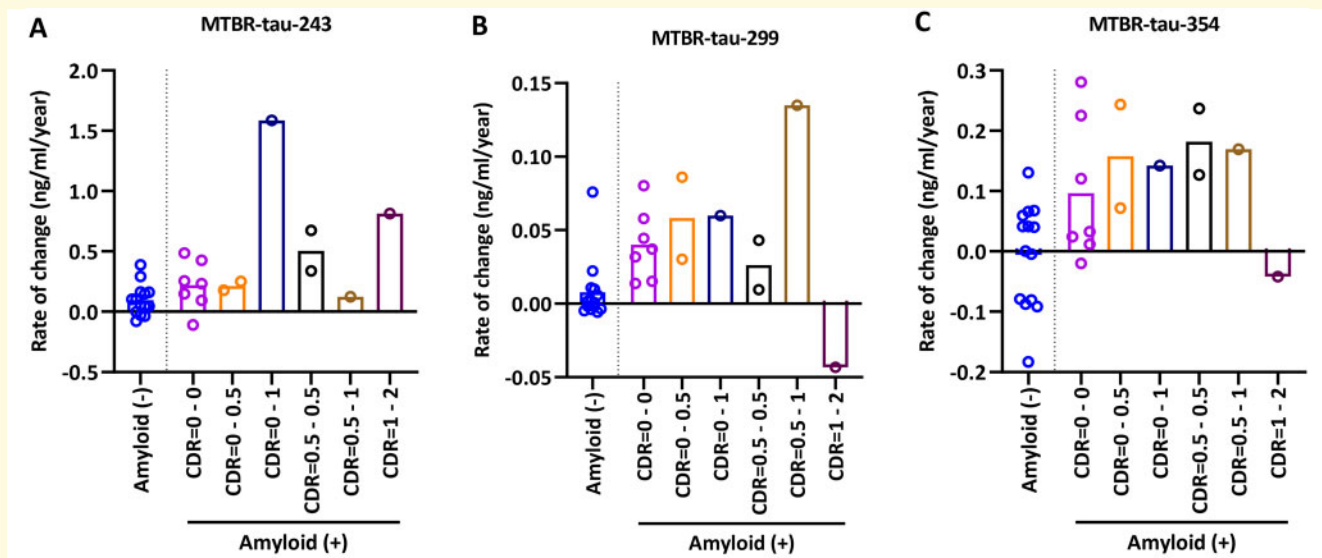
Figure 4 CSF MTBR-tau longitudinally increases with advancing Alzheimer's disease clinical stages. Longitudinal rates of changes (ng/ml/year) in (**A**) MTBR-tau-243, (**B**) MTBR-tau-299, and (**C**) MTBR-tau-354 in CSF in amyloid-negative (-) or positive (+) patients are shown (total $n = 28$ from longitudinal cohort). Amyloid-positive groups are further divided to various CDR changes including CDR = 0–0 ($n = 7$), CDR = 0–0.5 ($n = 2$), CDR = 0–1 ($n = 1$), CDR = 0.5–0.5 ($n = 2$), CDR = 0.5–1 ($n = 1$), and CDR = 1–2 ($n = 1$, Participant A). While the participants in the amyloid-negative group did not show significant longitudinal changes (as mean-values are close to zero), most participants in the amyloid-positive group showed increases in MTBR-tau concentrations longitudinally. Notably, Participant A with the greatest cognitive change after Alzheimer's disease clinical onset (CDR = 1 to 2) demonstrated only CSF MTBR-tau-243 increased with mild Alzheimer's disease (CDR = 1) to moderate Alzheimer's disease (CDR = 2) progression, while MTBR-tau-299 and 354 decreased.

pathological species may be present in the interstitial fluid (ISF) rather than CSF (Colin *et al.*, 2020). Although some reports revealed that CSF tau originates mainly from ISF (Reiber, 2001) and human CSF from Alzheimer's disease patients can induce tau seeding in a transgenic mice model (Skachokova *et al.*, 2019), further investigations are necessary to address if tau species detected in CSF reflect pathological tau which can propagate in human brain.

Previous studies show that inoculation with Alzheimer's disease brain tau aggregates into mouse brain induced severe tau pathology (Guo *et al.*, 2016; Narasimhan *et al.*, 2017); however, there have been no reports that identify the pathological tau species within the extracellular space that is also linked to disease progression in humans. This led us to test whether CSF MTBR-tau species change in Alzheimer's disease, and explore their suitability as novel Alzheimer's disease biomarkers. We found that CSF MTBR-tau levels are elevated in Alzheimer's disease and are consistent with species enriched in Alzheimer's disease brain insoluble fractions. Our finding that CSF MTBR-tau correlates with Alzheimer's disease clinical stage and tau pathology suggests that MTBR-tau is related to the mechanism of tau propagation in Alzheimer's disease, although the nature (i.e. monomeric, oligomeric, or fibril species) and origin of extracellular CSF MTBR-tau are still unknown. We hypothesize that CSF MTBR-tau may originate from brain aggregates or from neurons that actively secrete a monomeric species, and future studies should be designed to address this issue.

Interestingly, we found that the trajectories of the change in CSF MTBR-tau species were distinct across different regions of the MTBR and at each clinical stage of Alzheimer's disease. We posit that this finding is due to structural changes in tau as determined by recent cryo-EM findings. Cryo-EM analysis suggests the ordered β-sheet core of tau aggregates begins at residue 306 (Fitzpatrick *et al.*, 2017). Thus, MTBR-tau-354 (containing residue 354-369), MTBR-tau-299 (containing residue 299-317) and MTBR-tau-243 (containing residue 243-254) represent the internal side, border, and external side of the filament core, respectively. In contrast to both MTBR-tau-354 and MTBR-tau-299, MTBR-tau-243 levels were incrementally greater across all disease stages. MTBR-tau-243 and the nearby region (i.e. residue 226-230) levels in CSF are also highly correlated with tau PET SUVR performance (Fig. 5 and Supplementary Table 4), which supports our hypothesis that MTBR-tau-243 and potentially the nearby region deposit into brain tau aggregates and are also secreted extracellularly (Supplementary Fig. 13).

Our findings that MTBR-tau highly correlates with Alzheimer's disease pathology and clinical progression stages provide important insights into promising targets for therapeutic anti-tau drugs to treat tauopathies. For example, a novel tau antibody, recognizing an epitope in the upstream region of MTBR (residue 235-250) demonstrated a significant and selective ability to mitigate tau seeding from Alzheimer's disease and progressive supranuclear palsy
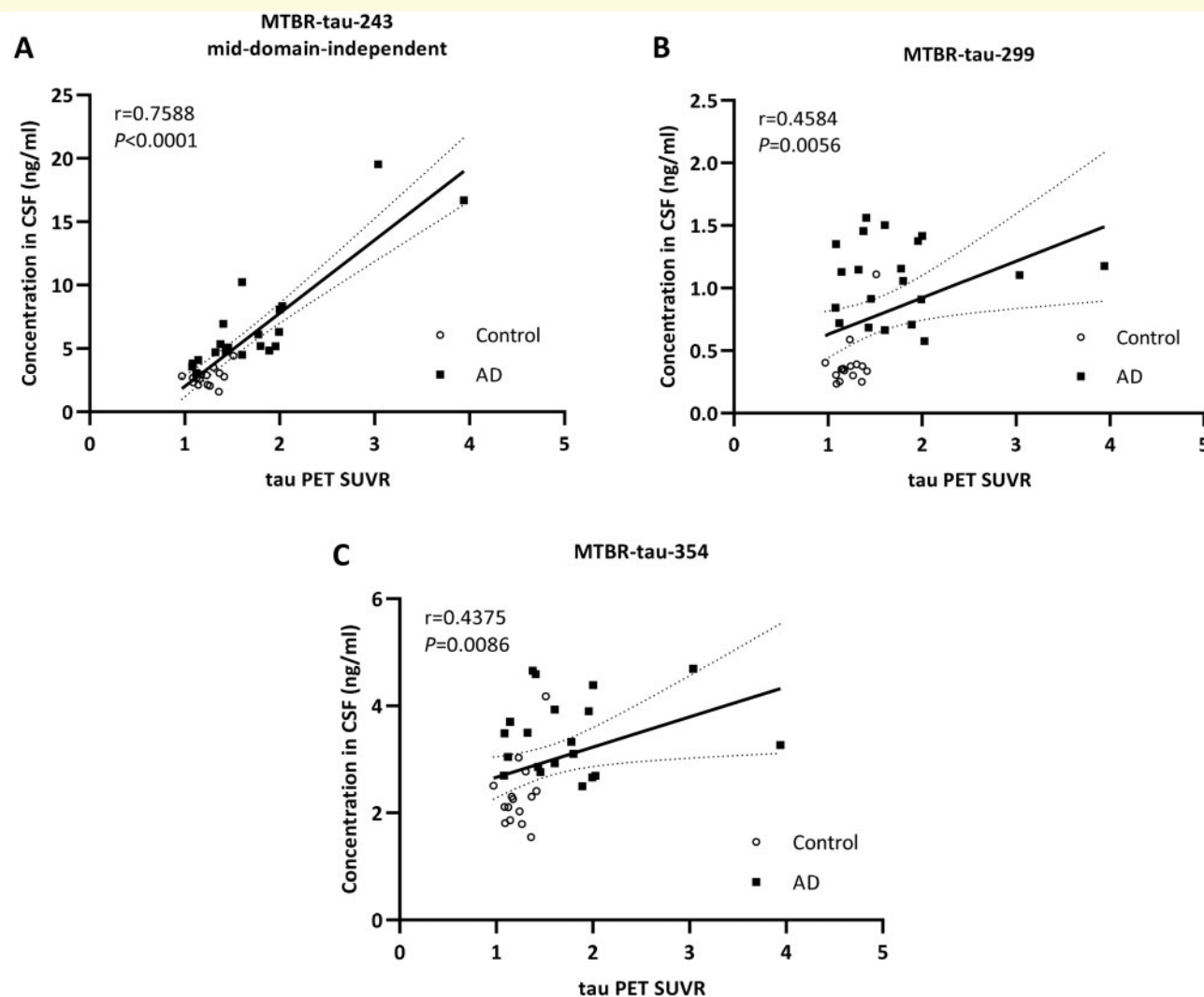
Figure 5 CSF MTBR-tau-243 is highly correlated with tau PET SUVR measure of tau tangles, while other MTBR-tau regions have low correlations with tau tangles. Correlations between tau PET (AV-1451) SUVR and mid-domain-independent (**A**) MTBR-tau-243, (**B**) MTBR-tau-299, and (**C**) MTBR-tau-354 concentrations in CSF are shown [control $n = 15$ and Alzheimer's disease (AD) $n = 20$ from tau PET cohort]. Open circle = control; filled squares = Alzheimer's disease. Mid-domain-independent MTBR-tau-243 showed the most significant correlation with tau PET SUVR ($r = 0.7588$, $P < 0.0001$).

brains in cell-based assays (Courade *et al.*, 2018). Their findings suggest that the upstream region of MTBR could be related to extracellular pathological tau. This is supported by the antibody mitigated propagation of tau pathology to distal brain regions in transgenic mice that had been injected with human Alzheimer's disease brain extracts (Albert *et al.*, 2019). Another novel tau antibody, recognizing an epitope in the upstream region of MTBR (residue 249-258) demonstrated the reduction of inducing tau pathology in cellular and *in vivo* transgenic mice models seeded by human Alzheimer's disease brain extracts (Vandermeeren *et al.*, 2018). Antibodies targeting MTBR-tau-299 and MTBR-tau-354 species also mitigated tau pathology induced by seeding of P301L tau or Alzheimer's disease brain extract (Weisová *et al.*, 2019; Roberts *et al.*, 2020), which supports the

hypothesis that species containing specific regions of MTBR are responsible for the spread of tau pathology in tauopathies.

In summary, we discovered that MTBR-tau species in CSF exist as C-terminal fragments and are specifically increased in Alzheimer's disease, reflecting the enrichment seen in Alzheimer's disease brain aggregates. Our findings suggest specific MTBR-containing species (MTBR-tau-299 and MTBR-tau-243) are promising CSF biomarkers to measure amyloid and tau pathology in Alzheimer's disease. In particular, the mid-domain-independent MTBR-tau-243 paralleled disease progression and tau pathology in Alzheimer's disease and may be utilized as a biomarker of tau pathology and a target for novel anti-tau antibody therapies.

Acknowledgements

Funding

Competing interests

K.H. is an Eisai-sponsored visiting researcher at Washington University and has received salary from Eisai. Washington University and R.J.B. have equity ownership interest in C2N Diagnostics and receive royalty income based on technology (stable isotope labelling kinetics and blood plasma assay) licensed by Washington University to C2N Diagnostics. R.J.B. receives income from C2N Diagnostics for serving on the scientific advisory board. R.J.B., N.R.B., K.H. and C.S. may receive income based on technology (methods of diagnosing Alzheimer's disease with phosphorylation changes) pending license by Washington University to C2N Diagnostics. Washington University, with K.H., N.R.B., C.S., and R.J.B. as co-inventors, have submitted the US provisional patent application 'Methods to detect novel tau isoforms in CSF and use thereof to track tau neuropathology in Alzheimer's disease and other tauopathies'. R.J.B. has received honoraria from AC Immune, Janssen, Pfizer and Roche as a speaker, from AC Immune, Amgen, Eisai, and Janssen as a consultant, and from Roche as an advisory board member.

Supplementary material

Supplementary material is available at *Brain* online.

References

Albert M, Mairet-Coello G, Danis C, Lieger S, Caillierez R, Carrier S, et al. Prevention of tau seeding and propagation by immunotherapy with a central tau epitope antibody. Brain J Neurol 2019; 142: 1736–50.

Arriagada PV, Growdon JH, Hedley-Whyte ET, Hyman BT. Neurofibrillary tangles but not senile plaques parallel duration and severity of Alzheimer's disease. Neurology 1992; 42: 631–9.

Barthélemy NR, Fenaille F, Hirtz C, Sergeant N, Schraen-Maschke S, Vialaret J, et al. Tau protein quantification in human cerebrospinal fluid by targeted mass spectrometry at high sequence coverage provides insights into its primary structure heterogeneity. J Proteome Res 2016a; 15: 667–76.

Barthélemy NR, Gabelle A, Hirtz C, Fenaille F, Sergeant N, Schraen-Maschke S, et al. Differential mass spectrometry profiles of tau protein in the cerebrospinal fluid of patients with Alzheimer's disease, progressive supranuclear palsy, and dementia with lewy bodies. J Alzheimers Dis 2016b; 51: 1033–43.

Barthélemy NR, Mallipeddi N, Moiseyev P, Sato C, Bateman RJ. Tau phosphorylation rates measured by mass spectrometry differ in the intracellular brain vs. extracellular cerebrospinal fluid compartments and are differentially affected by Alzheimer's disease. Front Aging Neurosci 2019; 11:121.

Bejanin A, Schonhaut DR, La Joie R, Kramer JH, Baker SL, Sosa N, et al. Tau pathology and neurodegeneration contribute to cognitive impairment in Alzheimer's disease. Brain J Neurol 2017; 140: 3286–300.

Benjamini Y, Hochberg Y. Controlling the false discovery rate: a practical and powerful approach to multiple testing. J R Stat Soc Ser B Methodol 1995; 57: 289–300.

Blennow K, Chen C, Cicognola C, Wildsmith KR, Manser PT, Bohorquez SMS, et al. Cerebrospinal fluid tau fragment correlates with tau PET: a candidate biomarker for tangle pathology. Brain 2020; 143: 650–60.

Chen H-H, Liu P, Auger P, Lee S-H, Adolfsson O, Rey-Bellet L, et al. Calpain-mediated tau fragmentation is altered in Alzheimer's disease progression. Sci Rep 2018; 8: 16725.

Cicognola C, Brinkmalm G, Wahlgren J, Portelius E, Gobom J, Cullen NC, et al. Novel tau fragments in cerebrospinal fluid: relation to tangle pathology and cognitive decline in Alzheimer's disease. Acta Neuropathol 2019; 137: 279–96.

Colin M, Dujardin S, Schraen-Maschke S, Meno-Tetang G, Duyckaerts C, Courade J-P, et al. From the prion-like propagation hypothesis to therapeutic strategies of anti-tau immunotherapy. Acta Neuropathol 2020; 139: 3–25.

Cotman CW, Poon WW, Rissman RA, Blurton-Jones M. The role of caspase cleavage of tau in Alzheimer disease neuropathology. J Neuropathol Exp Neurol 2005; 64: 104–12.

Courade J-P, Angers R, Mairet-Coello G, Pacico N, Tyson K, Lightwood D, et al. Epitope determines efficacy of therapeutic anti-Tau antibodies in a functional assay with human Alzheimer Tau. Acta Neuropathol 2018; 136: 729–45.

Falcon B, Zhang W, Murzin AG, Murshudov G, Garringer HJ, Vidal R, et al. Structures of filaments from Pick's disease reveal a novel tau protein fold. Nature 2018; 561: 137–40.

Falcon B, Zivanov J, Zhang W, Murzin AG, Garringer HJ, Vidal R, et al. Novel tau filament fold in chronic traumatic encephalopathy encloses hydrophobic molecules. Nature 2019; 568: 420–3.

Fitzpatrick AWP, Falcon B, He S, Murzin AG, Murshudov G, Garringer HJ, et al. Cryo-EM structures of tau filaments from Alzheimer's disease. Nature 2017; 547: 185–90.

Frost B, Jacks RL, Diamond MI. Propagation of tau misfolding from the outside to the inside of a cell. J Biol Chem 2009; 284: 12845–52.

Gamblin TC, Chen F, Zambrano A, Abraha A, Lagalwar S, Guillozet AL, et al. Caspase cleavage of tau: linking amyloid and

neurofibrillary tangles in Alzheimer's disease. Proc Natl Acad Sci USA 2003; 100: 10032–7.

Goedert M, Clavaguera F, Tolnay M. The propagation of prion-like protein inclusions in neurodegenerative diseases. Trends Neurosci 2010; 33: 317–25.

Goedert M, Eisenberg DS, Crowther RA. Propagation of tau aggregates and neurodegeneration. Annu Rev Neurosci 2017; 40: 189–210.

Gordon BA, Blazey TM, Christensen J, Dincer A, Flores S, Keefe S, et al. Tau PET in autosomal dominant Alzheimer's disease: relationship with cognition, dementia and other biomarkers. Brain 2019; 142: 1063–76.

Guo JL, Narasimhan S, Changolkar L, He Z, Stieber A, Zhang B, et al. Unique pathological tau conformers from Alzheimer's brains transmit tau pathology in nontransgenic mice. J Exp Med 2016; 213: 2635–54.

Jack CR, Wiste HJ, Schwarz CG, Lowe VJ, Senjem ML, Vemuri P, et al. Longitudinal tau PET in ageing and Alzheimer's disease. Brain 2018; 141: 1517–28.

Johnson KA, Schultz A, Betensky RA, Becker JA, Sepulcre J, Rentz D, et al. Tau PET imaging in aging and early Alzheimer's disease. Ann Neurol 2016; 79: 110–9.

Lasagna-Reeves CA, Castillo-Carranza DL, Sengupta U, Guerrero-Munoz MJ, Kiritoshi T, Neugebauer V, et al. Alzheimer brain-derived tau oligomers propagate pathology from endogenous tau. Sci Rep 2012; 2: 700.

Malia TJ, Teplyakov A, Ernst R, Wu S-J, Lacy ER, Liu X, et al. Epitope mapping and structural basis for the recognition of phosphorylated tau by the anti-tau antibody AT8. Proteins 2016; 84: 427–34.

Meredith JE, Sankaranarayanan S, Guss V, Lanzetti AJ, Berisha F, Neely RJ, et al. Characterization of novel CSF Tau and ptau biomarkers for Alzheimer's disease. PLoS One 2013; 8: e76523.

Mirbaha H, Chen D, Morazova OA, Ruff KM, Sharma AM, Liu X, et al. Inert and seed-competent tau monomers suggest structural origins of aggregation. eLife 2018; 7: e36584.

Narasimhan S, Guo JL, Changolkar L, Stieber A, McBride JD, Silva LV, et al. Pathological tau strains from human brains recapitulate the diversity of tauopathies in nontransgenic mouse brain. J Neurosci 2017; 37: 11406–23.

Neddens J, Temmel M, Flunkert S, Kerschbaumer B, Hoeller C, Loeffler T, et al. Phosphorylation of different tau sites during progression of Alzheimer's disease. Acta Neuropathol Commun 2018; 6: 52.

Ossenkoppele R, Schonhaut DR, Schöll M, Lockhart SN, Ayakta N, Baker SL, et al. Tau PET patterns mirror clinical and neuroanatomical variability in Alzheimer's disease. Brain 2016; 139: 1551–67.

Patterson BW, Elbert DL, Mawuenyega KG, Kasten T, Ovod V, Ma S, et al. Age and amyloid effects on human central nervous system amyloid-beta kinetics. Ann Neurol 2015; 78: 439–53.

Quinn JP, Corbett NJ, Kellett KAB, Hooper NM. Tau Proteolysis in the Pathogenesis of Tauopathies: neurotoxic Fragments and Novel Biomarkers. J Alzheimers Dis 2018; 63: 13–33.

Reiber H. Dynamics of brain-derived proteins in cerebrospinal fluid. Clin Chim Acta 2001; 310: 173–86.

Roberts M, Sevastou I, Imaizumi Y, Mistry K, Talma S, Dey M, et al. Pre-clinical characterisation of E2814, a high-affinity antibody targeting the microtubule-binding repeat domain of tau for passive immunotherapy in Alzheimer's disease. Acta Neuropathol Commun 2020; 8: 13.

Sanders DW, Kaufman SK, DeVos SL, Sharma AM, Mirbaha H, Li A, et al. Distinct tau prion strains propagate in cells and mice and define different tauopathies. Neuron 2014; 82: 1271–88.

Sato C, Barthélemy NR, Mawuenyega KG, Patterson BW, Gordon BA, Jockel-Balsarotti J, et al. Tau kinetics in neurons and the human central nervous system. Neuron 2018; 97: 1284–98.e7.

Skachokova Z, Martinisi A, Flach M, Sprenger F, Naegelin Y, Steiner-Monard V, et al. Cerebrospinal fluid from Alzheimer's disease patients promotes tau aggregation in transgenic mice. Acta Neuropathol Commun 2019; 7: 72.

Su Y, Blazey TM, Snyder AZ, Raichle ME, Marcus DS, Ances BM, et al. Partial volume correction in quantitative amyloid imaging. Neuroimage 2015; 107: 55–64.

Taniguchi-Watanabe S, Arai T, Kametani F, Nonaka T, Masuda-Suzukake M, Tarutani A, et al. Biochemical classification of tauopathies by immunoblot, protein sequence and mass spectrometric analyses of sarkosyl-insoluble and trypsin-resistant tau. Acta Neuropathol 2016; 131: 267–80.

Vandermeeren M, Borgers M, Van Kolen K, Theunis C, Vasconcelos B, Bottelbergs A, et al. Anti-tau monoclonal antibodies derived from soluble and filamentous tau show diverse functional properties in vitro and in vivo. J Alzheimers Dis 2018; 65: 265–81.

Weisová P, Cehlár O, Škrabana R, Žilková M, Filipčík P, Kováčech B, et al. Therapeutic antibody targeting microtubule-binding domain prevents neuronal internalization of extracellular tau via masking neuron surface proteoglycans. Acta Neuropathol Commun 2019; 7: 129.

Wu JW, Hussaini SA, Bastille IM, Rodriguez GA, Mrejeru A, Rilett K, et al. Neuronal activity enhances tau propagation and tau pathology in vivo. Nat Neurosci 2016; 19: 1085–92.

Zhang W, Tarutani A, Newell KL, Murzin AG, Matsubara T, Falcon B, et al. Novel tau filament fold in corticobasal degeneration. Nature 2020; 580: 283–7.

Zhang Z, Song M, Liu X, Kang SS, Kwon I-S, Duong DM, et al. Cleavage of tau by asparagine endopeptidase mediates the neurofibrillary pathology in Alzheimer's disease. Nat Med 2014; 20: 1254–62.

Zhao X, Kotilinek LA, Smith B, Hlynialuk C, Zahs K, Ramsden M, et al. Caspase-2 cleavage of tau reversibly impairs memory. Nat Med 2016; 22: 1268–76.